View metadata, citation and similar papers at core.ac.uk
brought to you by CORE
provided by Elsevier - Publisher Connector

Physics Letters B 695 (2011) 387–391
Contents lists available at ScienceDirect
Physics Letters B
www.elsevier.com/locate/physletb

Phase diagram of hot and dense QCD constrained by the Statistical Model

Kenji Fukushima

Yukawa Institute for Theoretical Physics, Kyoto University, Kyoto 606-8502, Japan

ARTICLE INFO

Article history:
Received 3 October 2010
Received in revised form 24 October 2010
Accepted 21 November 2010
Available online 25 November 2010
Editor: J.-P. Blaizot

Keywords:
Quark–gluon plasma
Dense QCD
Phase diagram

ABSTRACT

We propose a prescription to constrain the chiral effective model approach to the QCD phase diagram using the thermal Statistical Model which is a hadronic description consistent with the heavy-ion experimental data at the chemical freeze-out. In the transition region where thermal quantities of hadrons blow up, deconfined quarks and gluons should smoothly take over the relevant degrees of freedom from color confined hadrons. We use the Polyakov-loop coupled Nambu–Jona-Lasinio (PNJL) model as an effective description in the quark side. We require that the validity regions of these models should have an overlap on the phase diagram, which gives a condition to reduce model uncertainty. Our results favor a phase diagram with the chiral and the deconfinement phase transitions both staying close to the chemical freeze-out points until $\mu_B = 500$–600 MeV, above which the model parameter is not well constrained.

© 2010 Elsevier B.V. Open access under CC BY license.

1. Introduction

Exploration of the QCD (Quantum Chromodynamics) phase diagram, particularly toward higher baryon-density regime, is of increasing importance in both theoretical and experimental sides [1]. From the theoretical point of view, so far, only the lattice-QCD simulation [1,2] is the first-principle approach at work to the QCD phase transitions — chiral restoration and quark deconfinement. The functional renormalization group (RG) method is also developing as a promising non-perturbative tool [3,4] but has not been sufficiently matured yet in hot and dense QCD physics. The chiral condensate $\langle\bar{\psi}\psi\rangle$ and the Polyakov loop Φ are the (approximate) order parameters for chiral restoration and quark deconfinement, respectively, which are gauge invariant and measurable on the lattice. The lattice-QCD simulation is, however, of no practical use unless the baryon chemical potential μ_B is much smaller than the temperature T. For $\mu_B/T \gtrsim 1$ the notorious sign problem prevents us from extracting any reliable information from the lattice-QCD data [5].

The effective model study is an alternative and pragmatic approach toward the phase diagram of dense QCD. The essential idea is the following. It is next to impossible to attack hot and dense QCD directly in the transition region. One can build, instead, a model that is consistent with hadron properties in the vacuum and then extend the model description to finite-T and/or finite-μ_B environments. What is commonly recognized as the "QCD phase diagram" is actually a theoretical conjecture based on various effective-model studies [1,6]. Hence, the QCD phase diagram research by means of effective models must be guided and supplemented carefully by the consistency check with other data than the vacuum hadron properties.

Along this line the Polyakov-loop coupled chiral models such as the PNJL (Polyakov–Nambu–Jona-Lasinio) [7–11] and the PQM (Polyakov Quark–Meson) [12,13] models are successful to handle $\langle\bar{\psi}\psi\rangle$ and Φ on the equal footing. The important point is that the Polyakov-loop potential $\mathcal{U}[\Phi]$ can be determined by $\Phi(T)$ and the pressure $p(T)$ known from the lattice simulation of the pure-gluonic theory [14]. This means that the PNJL and PQM models include the pressure contribution from gluons as well as quarks, so that the models are able to deal with the full thermodynamics that is consistent with the full lattice-QCD simulation [8,12]. We note that the dynamics of transverse gluons A_i^T is also under the control of the deconfinement order parameter Φ and thus is to be incorporated in the Polyakov-loop potential $\mathcal{U}[\Phi]$, whereas Φ itself is expressed in terms of the longitudinal gluon A_4 alone.

Since the theoretical tool to examine $\langle\bar{\psi}\psi\rangle$ and Φ is now in our hands, it is intriguing to proceed to the next question; whether the chiral and the deconfinement phase transitions would go on simultaneously or separate after all when the baryon density is increasing. There are then two key issues. One is the so-called QCD (chiral) *critical point* (which is often called the *critical end-point*) at which the chiral and the baryon number susceptibilities diverge [15–17] and higher moments are even more singular [18]. The other one is a *triple-point-like region* associated with the appearance of hypothetical quarkyonic matter [19,20] where baryonic abundance surpasses mesonic one.

E-mail address: fuku@yukawa.kyoto-u.ac.jp.

0370-2693 © 2010 Elsevier B.V. Open access under CC BY license.
doi:10.1016/j.physletb.2010.11.040

One reasonable way to characterize quarkyonic matter for finite-N_c QCD is to use two order parameters; the Polyakov loop $\Phi = 0$ and the quark (baryon) number density $n_q = \langle \psi^\dagger \psi \rangle \neq 0$, which would definitely work for $N_c = \infty$ [19]. In principle this statement is not linked to chiral symmetry, but a substantially large value of n_q is favored by light quarks once chiral symmetric is restored. In this sense, practically, one can identify the quarkyonic phase as an exotic state where chiral symmetry is restored first (and thus n_q gets large) and, nevertheless, the confining property remains ($\Phi \simeq 0$). In other words the bulk pressure is mostly dominated by light quarks and only colored excitations near the Fermi surface feel a confining force. [There is also an argument that the confining force may cause inhomogeneous chiral condensation [21]. Such a possibility of spatial modulation [22] is beyond our current scope. In any case it is most unlikely that our present method would work for such a high density where inhomogeneous condensates are turned on.]

Phenomenological considerations could, however, lead to a different scenario [23], though some suggestive arguments for the quarkyonic window have been reported [20,24] and some model studies are also supportive [7,9]. In general the PNJL and PQM models at the mean-field level shall favor the quarkyonic picture; the model predicts the deconfinement temperature weakly dependent on μ_B. The Polyakov loop tends to be small for any μ_B as long as T is vanishingly small, while the chiral condensate melts at high μ_B regardless of T. Such decoupling behavior is partly because the mean-field treatment implicitly assumes large N_c.

It is already successful to apply the RG improvement to include mesonic fluctuations in the phase diagram study [13,25]. The RG method with mesonic fluctuations is indispensable to look closely into properties at the QCD critical point. In contrast, the bulk structure of the QCD phase diagram is not affected qualitatively. It is still highly non-trivial how to take account of other fluctuations such as the baryonic contribution and the quark-loop effects on the Polyakov-loop potential. In this respect the observation in Ref. [12] is the most interesting and even surprising. They postulated a μ_B-dependent form of $\mathcal{U}[\Phi]$ and found that it leads to a qualitative change on the phase diagram. We note that not μ_B- but T-dependence in $\mathcal{U}[\Phi]$ would be much less harmful since $\mathcal{U}[\Phi]$ at $\mu_B = 0$ is constrained anyway by the lattice data as already mentioned. It is thus extremely important to select a proper choice out for μ_B-dependent $\mathcal{U}[\Phi]$. This work is an attempt to approach this problem from the phenomenological point of view.

2. Thermodynamics from the Statistical Model

Regarding the QCD phase diagram at finite T and μ_B useful information is quite limited. Only the chemical freeze-out points in the heavy-ion collisions are experimental hints about the phase diagram. Although the freeze-out points shape an intriguing curve on the μ_B–T plane, as plotted by error-bar dots in Fig. 1, one should carefully treat them.

The freeze-out points are not direct experimental data but *an* interpretation through the Statistical Model [26,27]. In view of the fact that the Statistical Model is such successful to fit various particle ratios with μ_B and T only (other parameters μ_Q, μ_s, and μ_c are determined by the collision condition), it is legitimate to take the freeze-out points for experimental data, which in turn validates the Statistical Model, though why it works lacks for an explanation. In particular baryons should interact strongly at high density, and nevertheless, it seems that the Statistical Model works for the particle ratio even near $\mu_B \sim 800$ MeV. We do not try to theoretically justify the Statistical Model here, but simply make use of it

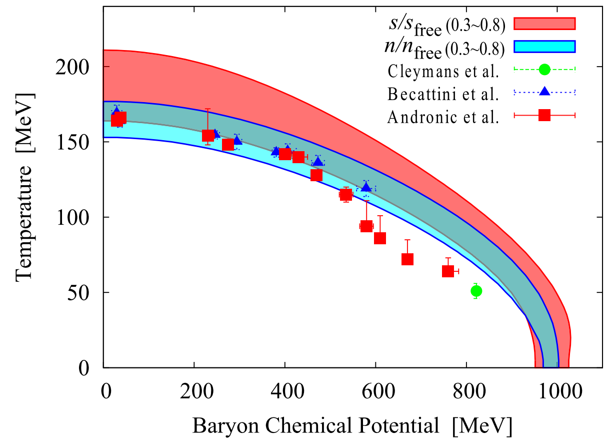

Fig. 1. Chemical freeze-out points taken from Refs. [20,26,27]. The red and blue (upper and lower) bands represent the regions where the entropy density s and the baryon number density n_B, respectively, increase quickly from 0.3 to 0.8 in the unit of free quark–gluon values, $s_{\rm free}$ and $n_{\rm free}$ (see Eq. (1)). (For interpretation of the references to color in this figure legend, the reader is referred to the web version of this Letter.)

accepting that it is anyway a description consistent with the experimental observation.

It is then a straightforward application of the Statistical Model to estimate thermodynamic quantities such as the pressure p, the entropy density s, and the baryon number density n_B as functions of T and μ_B. We here utilize an open code *THERMUS* ver.2.1 to calculate s and n_B [28].

Fig. 1 shows s and n_B from *THERMUS* together with the chemical freeze-out points taken from Refs. [20,26,27]. For convenience we normalized s and n_B by

$$s_{\rm free} = \left\{ (N_c^2 - 1) + \frac{7}{4} N_c N_f \right\} \frac{4\pi^2}{45} T^3 + \frac{N_c N_f}{3} \mu_q^2 T,$$
$$n_{\rm free} = N_f \left(\frac{\mu_q^3}{3\pi^2} + \frac{\mu_q T^2}{3} \right). \qquad (1)$$

These are the entropy density and the baryon number density of free massless $N_c^2 - 1$ gluons and $N_c N_f$ quarks.

Here we note that, in drawing Fig. 1, we have intentionally relaxed the neutrality conditions for electric charge and heavy flavors and simply set $\mu_Q = \mu_s = \mu_c = 0$. We have done so to make it easier to compare the results from the Statistical Model to the chiral effective model approach in later discussions. [We note that one can force the chiral models to satisfy neutrality but it would be technically involved and, besides, its effect on the phase diagram is minor [29].]

We used Eq. (1) with $N_c = N_f = 3$. We should note that the choice of $s_{\rm free}$ and $n_{\rm free}$ is (reasonable but) arbitrary and the following discussions do not rely on this choice at all. These $s_{\rm free}$ and $n_{\rm free}$ are just common denominators to display the Statistical Model and the PNJL model results.

The Statistical Model cannot tell us about the QCD phase transitions. Still, Fig. 1 is suggestive enough. We can clearly see the thermodynamic quantities from the Statistical Model blowing up in a relatively narrow region. [Strictly speaking, they do not blow up, but just increase significantly.] Two bands indicate where $s/s_{\rm free}$ (upper red) and $n_B/n_{\rm free}$ (lower blue) grow quickly from 0.3 to 0.8. In the Hagedorn's picture [30] this rapid and simultaneous rise in s and n_B may have a natural interpretation as the Hagedorn limiting temperature, above which color degrees of freedom is liberated, i.e. deconfinement takes place.

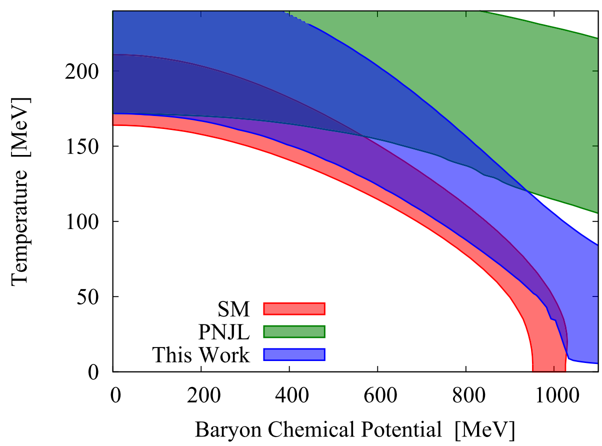

Fig. 2. Entropy density normalized by s_{free} (from 0.3 to 0.8) in the Statistical Model (bottom band with red color; same as shown in Fig. 1) and that in the PNJL model with a choice $T_0 = 200$ MeV (top band with green color). The blue band between two represents the results with the ansatz (4). (For interpretation of the references to color in this figure legend, the reader is referred to the web version of this Letter.)

3. Thermodynamics from the PNJL model

Fig. 1 is useful to have a guess-estimate about the deconfinement boundary but we can deduce no information about the chiral transition. Thus, to address the QCD phase transitions, we must find another way to connect the thermodynamics in Fig. 1 to the order parameters $\langle\bar{\psi}\psi\rangle$ and Φ. Let us go into details of the chiral effective model for that purpose.

It is essential to adopt the Polyakov-loop augmented model here because the entropy density should contain the contribution from gluons which is taken care of by $\mathcal{U}[\Phi]$. The PNJL model that we use in what follows is defined with the following potential:

$$\mathcal{U}[\Phi,\bar{\Phi}] = T^4\biggl\{-\frac{a(T)}{2}\bar{\Phi}\Phi + b(T)\ln\bigl[1-6\bar{\Phi}\Phi+4\bigl(\bar{\Phi}^3+\Phi^3\bigr)-3(\bar{\Phi}\Phi)^2\bigr]\biggr\} \tag{2}$$

with $a(T) = a_0 + a_1(T_0/T) + a_2(T_0/T)^2$ and $b(T) = b_3(T_0/T)^3$. There are five parameters one out of which is fixed by the Stefan–Boltzmann law. Other parameters are determined by the pure-gluonic lattice data as $a_0 = 3.51$, $a_1 = -2.47$, $a_2 = 15.2$, $b_3 = -1.75$, and $T_0 = 270$ MeV [8]. It is important to note that only T_0 is a parameter with the mass dimension, so that the energy scale in the gluon dynamics is set by this T_0.

In addition, the NJL sector of the PNJL model has five more parameters in the three-flavor case [7]; the light and heavy quark masses m_{ud} and m_{s}, the momentum cutoff Λ, the four-fermionic interaction strength g_{s}, and the $U(1)_{\text{A}}$-breaking six-fermionic interaction strength g_{d}, which are all fixed by the pion mass m_π, the kaon mass m_K, the eta-prime mass $m_{\eta'}$, the pion decay constant f_π, and the chiral condensate $\langle\bar{\psi}\psi\rangle$ [31].

In the presence of dynamical quarks, if we keep using $T_0 = 270$ MeV, the simultaneous crossover temperature of deconfinement and chiral restoration is above 200 MeV, which is too high as compared to the lattice-QCD value. This problem has been nicely resolved in Ref. [12]; the back-reaction from quark loops affects the mass scale to change from $T_0 = 270$ MeV for $N_{\text{f}} = 0$ down to $T_0 = 208$ MeV for $N_{\text{f}} = 2$, and $T_0 = 187$ MeV for $N_{\text{f}} = 2+1$ [12]. In this work we choose to use $T_0 = 200$ MeV throughout; our aim here is to propose an idea and test it qualitatively, but not to come to quantitative details.

In Fig. 2 we show the entropy density calculated in the mean-field PNJL model with $T_0 = 200$ MeV in the same way as presented in Fig. 1. The bottom (top) band in red (green) color is the result from the Statistical Model (PNJL model). From the figure it is obvious that the naive PNJL model cannot pass the consistency check with the Statistical Model for large μ_{B}. Even for $\mu_{\text{B}}/T \ll 1$ we see that the curvature of the band curve is significantly different; the PNJL model result is too flat horizontally (as suggested in the large-N_{c} argument).

4. Problem and ansatz

Such a manifest discrepancy between the Statistical Model and the PNJL model is a crucial problem in the QCD phase diagram research. This problem cannot be resolved even in the RG improved PQM model because the baryonic excitations are still missing. To make the entropy density get saturated for $\mu_{\text{B}} \gtrsim 400$ MeV, baryonic degrees of freedom must be released at smaller temperature than predicted by the PNJL model. One can understand this problem in a more intuitive way too. That is, the color-singlet contribution in the partition function involves the following integration:

$$\int d^3k\, f\bigl(e^{-N_{\text{c}}(\sqrt{k^2+M_{\text{q}}^2}-\mu_{\text{q}})/T}\bigr) = \frac{1}{N_{\text{c}}^3}\int d^3k\, f\bigl(e^{-(\sqrt{k^2+M_{\text{B}}^2}-\mu_{\text{B}})/T}\bigr), \tag{3}$$

where f is an arbitrary function. The left-hand side represents the N_{c}-quark contribution and $M_{\text{B}} = N_{\text{c}}M_{\text{q}}$ and $\mu_{\text{B}} = N_{\text{c}}\mu_{\text{q}}$ in the right-hand side. Then it is clear that the vanishing Polyakov loop allows for only the color-singlet N_{c}-quark contribution in the PNJL-type model but such contribution like Eq. (3) underestimates the genuine baryonic excitation by a factor $1/N_{\text{c}}^3$. [In reality the situation should be better than this because repulsive interactions between baryons would reduce the baryon density as compared to the free case.]

Also there is another way to think about the mismatch between the Statistical Model and the PNJL model. The energy scale in the pure-gluonic sector in the PNJL setup is specified by one parameter T_0 that may change depending on T and μ_{B} as a result of the quark-loop effect. We have shifted T_0 from 270 MeV down to 200 MeV through which we have incorporated the scale change induced by thermal quarks. In this way we may well consider that $T_0(\mu_{\text{B}})$ should decrease with increasing μ_{B}, as was first pointed out in Ref. [12].

Our idea here is to make use of Fig. 2 to fix $T_0(\mu_{\text{B}})$ in such a way to be consist with the Statistical Model (or the output from *THERMUS* more specifically). One could have picked up other thermodynamic quantities than the entropy density, which would make little difference in the final result. In Ref. [26] the freeze-out curve is parametrized as $T_{\text{f}}(\mu_{\text{B}}) = a - b\mu_{\text{B}}^2 - c\mu_{\text{B}}^4$ with the fitting result $a = 166(2)$ MeV, $b = 1.39(16)\times 10^{-4}$ MeV^{-1}, and $c = 5.3(21)\times 10^{-11}$ MeV^{-3}. Because the behavior of the entropy density is dominantly controlled by deconfinement (in the PNJL model), we postulate that $T_0(\mu_{\text{B}})$ is to be correlated with $T_{\text{f}}(\mu_{\text{B}})$. Let us simply try to use the same b and make an ansatz as

$$\frac{T_0(\mu_{\text{B}})}{T_0} = 1-(bT_0)\left(\frac{\mu_{\text{B}}}{T_0}\right)^2 = 1-2.78\times 10^{-2}\left(\frac{\mu_{\text{B}}}{T_0}\right)^2, \tag{4}$$

which yields the blue band in the middle of Fig. 2. Here T_0 in the denominator is $T_0(\mu_{\text{B}}=0)$. We remark that we have set a technical lower bound $T_0(\mu_{\text{B}}) \geqslant 10$ MeV to prevent unphysical negative $T_0(\mu_{\text{B}})$ for large μ_{B}. In any case the validity of our ansatz (4) should be lost at such large μ_{B}. We see at a glance that the results

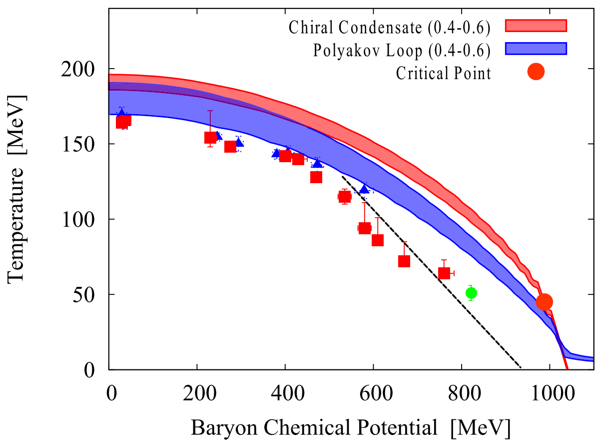

Fig. 3. Phase boundaries associated with deconfinement (lower blue band) and chiral restoration (upper red band). Each band represents a region where the (normalized) order parameter develops from 0.4 to 0.6. (For interpretation of the references to color in this figure legend, the reader is referred to the web version of this Letter.)

from this modified PNJL model have a reasonable overlap with the Statistical Model in the whole density region.

We would emphasize that it is naturally $\mathcal{U}[\Phi]$ that should be modified. As we have discussed below Eq. (3), the lack of baryonic degrees of freedom is attributed to the absence of confinement. Whether confined baryons or deconfined quarks are relevant is characterized by Φ in principle. Therefore the baryonic abundance at finite μ_B is to be linked to Φ. This in turn results in non-perturbative μ_B-dependence in the potential energy in terms of Φ. In the perturbative manner one can also understand how the μ_B-dependence enters $\mathcal{U}[\Phi]$; the loop diagram of the dressed *gluon* propagator with μ_B-dependent screening mass (i.e. quark–antiquark polarization) yields μ_B-dependent $\mathcal{U}[\Phi]$. We note here that the μ_B-dependence from the *quark* loop is already incorporated in the PNJL coupling.

Finally we point out that our choice in Eq. (4) happens to be very close to the independent argument in Ref. [12], in which the μ_B-dependence has been estimated from the running coupling constant as $T_0(\mu_B) = T_\tau\, e^{-1/(a_0 b(\mu_B))}$ which is expanded numerically to be $T_0(\mu_B)/T_0 \simeq 1 - 2.1 \times 10^{-2}(\mu_B/T_0)^2 + \cdots$. This similarity is quite indicative of justification.

5. Phase diagram and discussions

Now we get ready to draw a likely candidate for the QCD phase diagram that is consistent with the Statistical Model thermodynamics. Using the standard computational procedure of the mean-field PNJL model (see Ref. [7] for technical details) we can solve $\langle\bar\psi\psi\rangle$ and Φ as functions of T and μ_B, from which the phase boundaries of chiral restoration and quark deconfinement can be located.

Fig. 3 shows the phase diagram from the modified PNJL model with the ansatz (4). The blue (red) band is a region where the Polyakov loop Φ (normalized light-quark chiral condensate $\langle\bar u u\rangle/\langle\bar u u\rangle_0$) increases from 0.4 to 0.6. In contrast to the standard PNJL model results, the phase boundaries here show that the chiral and the deconfinement transitions are almost parallel to each other, which agrees with the situation considered in Refs. [12,23]. We have found the critical point at $(\mu_B, T) \simeq (45\ \text{MeV}, 330\ \text{MeV})$, but we should not take the location seriously because it is easily affected by small changes in the model [7]. Nevertheless, it is a good news for the critical point search that the QCD phase boundaries become closer to the chemical freeze-out curve, for the experimental signature would be detectable only if the fluctuation at freeze-out reflects the singular nature of criticality.

It is an intriguing observation that the chiral phase transition may occur (slightly) later than deconfinement. This is consistent with the Statistical Model assumption. In the Statistical Model the hadron masses are just the vacuum values and any hadron mass/width modification is neglected, which would be easily justified if the chiral phase transition takes place later than the Hagedorn temperature. Under such a phase structure, besides, our assumption of neglecting μ_B-dependence in the NJL-model parameters is as acceptable as the Statistical Model. We can say so because the NJL part mainly takes care of the hadron properties and the chiral dynamics which are intact in the Statistical Model.

Here we should state that the present study loses its validity around $\mu_B = 500$–600 MeV. This is because the chemical freeze-out temperatures in such high-density regions are far below the phase boundaries in Fig. 3 and the (not theoretical but experimental) validity of the Statistical Model is guaranteed up to the freeze-out points. For a guide to eyes, we draw a dashed line in Fig. 3 which limits the validity of the present approach. The fact that the phase boundaries from the model come far above the validity limit for $\mu_B \gtrsim 500$ MeV may indicate that the ansatz (4) breaks down or that a new state of matter exists there [20].

In the future it is an important question how our phenomenological ansatz (4) is validated/invalidated from the first-principle QCD calculation, which will be possibly answered by the functional RG method [4]. In any case, the most important message in this work is that it is unavoidable to think of μ_B-dependent $\mathcal{U}[\Phi]$; otherwise the results cannot fulfill the consistency with the Statistical Model in small-μ_B regions. Our ansatz (4) might need more refinement, but the *idea* to test the consistency-check at finite μ_B using the thermal Statistical Model is one principle to guide future developments in the QCD phase diagram research.

Finally, to avoid misunderstanding and make our assertion clear, we reiterate that the central point in this work is neither the ansatz (4) nor the phase diagram in Fig. 3 but the idea to match the chiral effective model and the thermal Statistical Model. The ansatz (4) is a simple example that can satisfy this requirement from the Statistical Model and Figs. 2 and 3 are demonstrations.

Acknowledgements

The author thanks Y. Hidaka for numerical assistance. He also thanks K. Redlich and J.M. Pawlowski for discussions and A. Andronic for the numerical data of his freeze-out points. This work is supported by Japanese MEXT grant No. 20740134 and in part by Yukawa International Program for Quark Hadron Sciences.

References

[1] For a recent review on the QCD phase diagram, see: K. Fukushima, T. Hatsuda, arXiv:1005.4814 [hep-ph].
[2] C. DeTar, U.M. Heller, Eur. Phys. J. A 41 (2009) 405.
[3] For a review on the functional RG for gauge theories, see: H. Gies, arXiv:hep-ph/0611146.
[4] J. Braun, H. Gies, J.M. Pawlowski, Phys. Lett. B 684 (2010) 262;
J. Braun, L.M. Haas, F. Marhauser, J.M. Pawlowski, arXiv:0908.0008 [hep-ph].
[5] For reviews on dense QCD and the sign problem, see: S. Muroya, A. Nakamura, C. Nonaka, T. Takaishi, Prog. Theor. Phys. 110 (2003) 615;
P. de Forcrand, PoS LAT2009 (2009) 010.
[6] K. Fukushima, J. Phys. G 35 (2008) 104020.
[7] K. Fukushima, Phys. Lett. B 591 (2004) 277;
K. Fukushima, Phys. Rev. D 77 (2008) 114028.
[8] C. Ratti, M.A. Thaler, W. Weise, Phys. Rev. D 73 (2006) 014019;
S. Roessner, C. Ratti, W. Weise, Phys. Rev. D 75 (2007) 034007.
[9] C. Sasaki, B. Friman, K. Redlich, Phys. Rev. D 75 (2007) 074013;
L. McLerran, K. Redlich, C. Sasaki, Nucl. Phys. A 824 (2009) 86.

[10] M. Ciminale, R. Gatto, N.D. Ippolito, G. Nardulli, M. Ruggieri, Phys. Rev. D 77 (2008) 054023.
[11] W.j. Fu, Z. Zhang, Y.x. Liu, Phys. Rev. D 77 (2008) 014006.
[12] B.J. Schaefer, J.M. Pawlowski, J. Wambach, Phys. Rev. D 76 (2007) 074023; B.J. Schaefer, M. Wagner, J. Wambach, Phys. Rev. D 81 (2010) 074013.
[13] V. Skokov, B. Stokic, B. Friman, K. Redlich, Phys. Rev. C 82 (2010) 015206; V. Skokov, B. Friman, K. Redlich, arXiv:1008.4570 [hep-ph].
[14] G. Boyd, J. Engels, F. Karsch, E. Laermann, C. Legeland, M. Lutgemeier, B. Petersson, Nucl. Phys. B 469 (1996) 419.
[15] M. Asakawa, K. Yazaki, Nucl. Phys. A 504 (1989) 668; A. Barducci, R. Casalbuoni, S. De Curtis, R. Gatto, G. Pettini, Phys. Lett. B 231 (1989) 463.
[16] M.A. Stephanov, K. Rajagopal, E.V. Shuryak, Phys. Rev. Lett. 81 (1998) 4816; M.A. Stephanov, K. Rajagopal, E.V. Shuryak, Phys. Rev. D 60 (1999) 114028.
[17] D.T. Son, M.A. Stephanov, Phys. Rev. D 70 (2004) 056001; H. Fujii, M. Ohtani, Phys. Rev. D 70 (2004) 014016.
[18] M.A. Stephanov, Phys. Rev. Lett. 102 (2009) 032301.
[19] L. McLerran, R.D. Pisarski, Nucl. Phys. A 796 (2007) 83.
[20] A. Andronic, et al., Nucl. Phys. A 837 (2010) 65.
[21] T. Kojo, Y. Hidaka, L. McLerran, R.D. Pisarski, Nucl. Phys. A 843 (2010) 37.
[22] E. Nakano, T. Tatsumi, Phys. Rev. D 71 (2005) 114006; D. Nickel, Phys. Rev. Lett. 103 (2009) 072301; D. Nickel, Phys. Rev. D 80 (2009) 074025.
[23] P. Castorina, R.V. Gavai, H. Satz, arXiv:1003.6078 [hep-ph].
[24] S. Hands, S. Kim, J.I. Skullerud, Phys. Rev. D 81 (2010) 091502.
[25] B.J. Schaefer, J. Wambach, Nucl. Phys. A 757 (2005) 479; B.J. Schaefer, J. Wambach, Phys. Rev. D 75 (2007) 085015.
[26] J. Cleymans, H. Oeschler, K. Redlich, S. Wheaton, Phys. Rev. C 73 (2006) 034905.
[27] F. Becattini, J. Manninen, M. Gazdzicki, Phys. Rev. C 73 (2006) 044905; A. Andronic, P. Braun-Munzinger, J. Stachel, Phys. Lett. B 673 (2009) 142.
[28] S. Wheaton, J. Cleymans, Comput. Phys. Commun. 180 (2009) 84.
[29] K. Fukushima, Phys. Rev. D 79 (2009) 074015.
[30] N. Cabibbo, G. Parisi, Phys. Lett. B 59 (1975) 67.
[31] T. Hatsuda, T. Kunihiro, Phys. Rep. 247 (1994) 221.